frontiers | Frontiers in Biomaterials Science

TYPE Original Research
PUBLISHED 17 April 2023
DOI 10.3389/fbiom.2023.1155919

OPEN ACCESS

EDITED BY
Elena Marcello,
Polytechnic University of Turin, Italy

REVIEWED BY
Berivan Cecen,
Rowan University, United States
Pooja Basnett,
University of Westminster,
United Kingdom

*CORRESPONDENCE
Darcy E. Wagner,
darcy.wagner@med.lu.se

SPECIALTY SECTION
This article was submitted to Biomaterials Science for Regenerative Therapies, a section of the journal Frontiers in Biomaterials Science

RECEIVED 31 January 2023
ACCEPTED 29 March 2023
PUBLISHED 17 April 2023

CITATION
Da Silva IA, Gvazava N, Putra Wendi I, Guinea R, García Giménez F, Stegmayr J, Klementieva O and Wagner DE (2023), Formalin-free fixation and xylene-free tissue processing preserves cell-hydrogel interactions for histological evaluation of 3D calcium alginate tissue engineered constructs.
Front. Front. Biomater. Sci. 2:1155919.
doi: 10.3389/fbiom.2023.1155919

Formalin-free fixation and xylene-free tissue processing preserves cell-hydrogel interactions for histological evaluation of 3D calcium alginate tissue engineered constructs

Iran Augusto Da Silva[1,2,3,4], Nika Gvazava[1,2,3,4], Indra Putra Wendi[1,2,3,4], Rodrigo Guinea[1,2,3,4], Francisco García Giménez[1,2,3,4,5], John Stegmayr[1,2,3,4], Oxana Klementieva[4,6] and Darcy E. Wagner[1,2,3,4]*

[1]Lung Bioengineering and Regeneration, Department of Experimental Medicine, Faculty of Medicine, Lund University, Lund, Sweden, [2]Wallenberg Center for Molecular Medicine, Faculty of Medicine, Lund University, Lund, Sweden, [3]Lund Stem Cell Center, Faculty of Medicine, Lund University, Lund, Sweden, [4]NanoLund, Lund University, Lund, Sweden, [5]Advanced Therapies in Biomedicine, Faculty of Experimental Sciences, Universidad Francisco de Vitoria, Madrid, Spain, [6]Medical Microspectroscopy, Department of Experimental Medicine, Faculty of Medicine, Lund University, Lund, Sweden

Histological evaluation of tissue-engineered products, including hydrogels for cellular encapsulation, is a critical and invaluable tool for assessing the product across multiple stages of its lifecycle from manufacture to implantation. However, many tissue-engineered products are comprised of polymers and hydrogels which are not optimized for use with conventional methods of tissue fixation and histological processing. Routine histology utilizes a combination of chemical fixatives, such as formaldehyde, and solvents such as xylene which have been optimized for use with native biological tissues due to their high protein and lipid content. Previous work has highlighted the challenges associated with processing hydrogels for routine histology due to their high water content and lack of diverse chemical moieties amenable for tissue fixation with traditional fixatives. Thus, hydrogel-based tissue engineering products are prone to histological artifacts during their validation which can lead to challenges in correctly interpreting results. In addition, chemicals used in conventional histological approaches are associated with significant health and environmental concerns due to their toxicity and there is thus an urgent need to identify suitable replacements. Here we use a multifactorial design of experiments approach to identify processing parameters capable of preserving cell-biomaterial interactions in a prototypical hydrogel system: ionically crosslinked calcium alginate. We identify a formalin free fixative which better retains cell-biomaterial interactions and calcium alginate hydrogel integrity as compared to the state-of-the-art formalin-based approaches. In addition, we demonstrate that this approach is compatible with a diversity of manufacturing techniques used to fabricate calcium alginate-based scaffolds for tissue engineering and cell therapy, including histological evaluation of cellular encapsulation in 3D tubes and thin tissue engineering scaffolds (~50 µm). Furthermore, we show that formalin-free fixation can be used to retain cell-biomaterial interactions and hydrogel architecture in hybrid

alginate-gelatin based scaffolds for use with histology and scanning electron microscopy. Taken together, these findings are a significant step forward towards improving histological evaluation of ionically crosslinked calcium alginate hydrogels and help make their validation less toxic, thus more environmentally friendly and sustainable.

KEYWORDS

alginate (PubChem CID: 91666324), tissue fixation, green histology, hydrogel, formalin-free, green lab, xylene-free

Introduction

Owing to their similarity to the native extracellular matrix (ECM), a diversity of hydrogel materials are under investigation for use in a wide range of regenerative medicine therapies, controlled release for drug delivery, as well as novel *in vitro* cell culture platforms (Hoffman, 2012; Caliari and Burdick, 2016). This includes the longstanding and prominent use of hydrogels as tissue engineering scaffolds for a range of tissues and organs as well as in cell therapy applications (e.g., cellular encapsulation into microspheres) (Nicodemus and Bryant, 2008). One of the most used hydrogel systems is based on alginate, a natural polymer derived from brown algae (Lee and Mooney, 2012; Abasalizadeh et al., 2020). In addition to its ability to be fabricated into diverse shapes using a variety of manufacturing approaches (e.g., microspheres, casting and 3D printing) (Aderibigbe and Buyana, 2018; Rastogi and Kandasubramanian, 2019; Uyen et al., 2020), alginate also offers the further advantage that many of these manufacturing processes can be performed under conditions which allow for cells to be incorporated into final crosslinked hydrogels with good viability (Jeon et al., 2019; De Santis et al., 2021). One of the most common forms of gel formation is through ionic crosslinking with divalent cations, most commonly calcium. While this crosslinking is reversible and known to be weak, it remains a highly attractive approach due to its relative simplicity and the fact that it supports cellular viability when exposure to divalent ions is short and with low concentrations (Cao et al., 2012). Ionically crosslinked alginate hydrogels have been extensively explored for regenerative medicine applications and drug delivery (Lee and Mooney, 2012).

As these technologies move closer to the clinic, one of the critical validation stages for their translation [e.g., as advanced therapy medical products (ATMPs in Europe)] is through *in vivo* transplantation studies. While several novel *in vivo* imaging modalities have recently been developed to non-invasively monitor the performance of cells and transplanted calcium alginate scaffolds (Arifin et al., 2019; Patrick et al., 2020), histological examination remains an invaluable and critical tool due to the fact that multiple, independent assessments can be made on a single sample. Further, a variety of biological molecules can be examined from histological sections and coupled to spatial information within the tissue. Histological examination also allows microscopic evaluation of host-biomaterial interactions as well as cell-biomaterial interactions at the molecular level. This is critical to assess the host immune response (e.g., foreign body response or integration with neighboring tissue) and the long-term survival and phenotype of transplanted cells. However, histological evaluation of alginate hydrogels is known to be challenging owing to their high-water content (Caliari and Burdick, 2016). Furthermore, ionically crosslinked alginate hydrogels are particularly challenging as they can quickly disintegrate during routine histological processing due to the use of incompatible chemicals and solvents (McGowan and Nagatomi, 2013). While histological evaluation of alginate hydrogels has been shown to be possible, it is known to be prone to artifacts such as loss of cells, distortion or loss of hydrogels, or detachment of implanted hydrogels from neighboring tissue upon implantation during routine histological processing using formalin fixation and xylene-based tissue processing (Bochenek et al., 2018; Somo et al., 2020).

Several different approaches have been reported in the literature thus far to enable histological assessment of alginate hydrogels and further to improve retention of the histological architecture of ionically crosslinked alginate hydrogels. The most used fixative agent is formaldehyde and neutral-buffered formalin is the most commonly utilized formulation (Jacobs-Tulleneers-Thevissen et al., 2013; Bochenek et al., 2018; Somo et al., 2020). Other buffers and physiological solutions have been described for formalin such as saline (Hunt et al., 2009), sodium cacodylate-barium chloride buffer (Guillaume et al., 2014) and Tris-buffered saline with added calcium (Khatab et al., 2020) as well as glutaraldehyde based fixation in phosphate buffer (Johnson et al., 2011). Barium crosslinking of calcium alginate hydrogels prior to treatment with neutral-buffered formalin has also shown promise in stabilizing hydrogels during routine histological processing (McGowan and Nagatomi, 2013). Barium, owing to its larger size, is known to form more stable ionic crosslinks than calcium ions (Mørch et al., 2006).

Alternatively, embedding materials [e.g., glycol methacrylate (GMA)] have been utilized and reported to improve histological processing of ionically crosslinked alginates (Fritschy et al., 1995; De Haan et al., 2002; James et al., 2004; McGowan and Nagatomi, 2013). While the initially described GMA-based methods contained toxic chemicals, new approaches have improved their occupational and environmental safety (Gerrits et al., 1991). However, polymerized GMA remains after sectioning and may interfere with downstream imaging processes and or make constructs processed using this approach incompatible with some microscopy and analytical methods (Yeung and Chan, 2014). Physical fixation techniques such as snap freezing (De Haan et al., 2002), optimal cutting temperature (OCT) embedding for cryosectioning, and lyophilization have also been used for histological processing of alginates for light microscopy and scanning electron microscopy (McGowan and Nagatomi, 2013; De Santis et al., 2021). However, these approaches are also associated with limitations as well as artifacts. For example, OCT embedding followed by cryosectioning and staining offers the advantage of generally preserving the tissue architecture, but optical resolution is more limited for histological evaluation. The lower optical resolution is due to the lack of optical

clearing, as which occurs for paraffin embedded samples during routine tissue processing, and challenges in generating thin sections as can be done with paraffin embedded samples for many tissues. This lower optical resolution can make interpretation and image processing more challenging. Thus, there is a need to identify alternative fixation and tissue processing approaches for histologically evaluating ionically crosslinked calcium alginates.

In recent years, there has been increased awareness of developing alternative processes which are more environmentally and occupationally safe for histological processing. Routine histological processing is known to contain several chemicals with both major health and environmental concerns. The main chemicals used in routine or conventional histological processing are formalin (formaldehyde-based fixation) and xylene in tissue processing. Formaldehyde (referred to as formalin when in an aqueous solution) is known to induce stable fixation when done under optimal settings (Metgud et al., 2013) but it is a known carcinogen (Cammalleri et al., 2022). On the other hand, xylene is used for tissue clearing (de-lipidation) as well as to allow for paraffin infiltration. Xylene is known to be acutely toxic for both humans and wildlife (e.g., aquatic life) and is an environmental pollutant (Rajan and Malathi, 2014). Due to these concerns and its high volume of usage, xylene is currently on the European Chemical Agency's "Community Rolling Action Plan (CoRAP)" which aims to evaluate substances of concern. There is thus a pressing need to identify sustainable strategies to replace these two main chemicals which are widely used in pathological laboratories around the world and are required for evaluating and validating potential regenerative medicine therapies. We recently described a xylene-free tissue processing protocol which substitutes isopropanol for xylene but was initially optimized for native biological (animal) tissue processing. We have additionally used this approach to histologically study cells seeded on polyester Transwell™ membranes as well as Matrigel based organoids (Alsafadi et al., 2022; Silva et al., 2022). However, most of the previous literature and our own previous work used formalin-based crosslinking in conjunction with xylene-free tissue processing. Therefore, whether alternative fixation processes are compatible with xylene-free tissue processing for processing of ionically crosslinked alginate remains unknown.

Here we sought to evaluate the potential of different commercially available fixatives, including a formalin-free formulation, for their capability of fixing both native biological tissues as well as ionically crosslinked calcium alginate hydrogels to preserve cell-biomaterial interactions. In addition, a main goal of this study was to evaluate if the entire histological process of native biological tissues and bioengineered tissues could be performed without the use of environmentally and occupationally hazardous chemicals (i.e., formalin-free green chemistry).

Materials and methods

Tissue harvest and precision tissue slice preparation

All experiments involving murine tissue was done with approval from the Malmö/Lund Ethics Committee on Animal Testing (M11908-19). As assessment of disease at the histological level was not the primary aim of the study, we utilized excess tissue available from mice scheduled to be euthanized for other studies [APP/PS1 mice (Jackson Labs, United States)]. Animals were anaesthetized *via* an intraperitoneal injection of sodium pentobarbital (40–50 mg/kg) followed by transcardial perfusion with ~20 mL of oxygenated (carbogen, 5% CO_2, 95% O_2) artificial cerebrospinal fluid (aCSF) as we described previously (Gvazava et al., 2023). aCSF was comprised of (in mM): 92 *N*-methyl-D-glucamine (NMDG), 2.5 KCl, 1.25 NaH_2PO_4, 30 $NaHCO_3$, 20 HEPES, 25 glucose, 2 thiourea, 5 Na-ascorbate, 3 Na-pyruvate, 0.5 $CaCl_2{\cdot}2H_2O$, and 10 $MgSO_4{\cdot}7H_2O$. pH was titrated to 7.3–7.4 with 37% hydrochloric acid (~7 ± 0.2 mL).

Brain slices containing perirhinal cortex and hippocampus were prepared at 275 µm thickness using a vibratome (Leica VT1200 S, Wetzlar, Germany). All other tissues were sectioned to 200 µm thickness using a 7000SMZ-2 Vibrotome (Campden Instruments, Ltd.). Tissue was then fixed overnight with one of 4 fixatives: 10% neutral-buffered formalin (NBF) (HT501128-4L Sigma-Aldrich, Sweden), formalin free fixative (A5472-1GAL Sigma-Aldrich, United States), 4% PFA in 0.1 M phosphate buffer (HL96753, Histolab AB, Sweden), or 2.0% electron microscopy grade glutaraldehyde (G5882-100 ML Sigma-Aldrich) in 0.42x PBS (1x PBS, 10 mM PO_4^{3-}, 18912014 Thermo Scientific, Sweden), 0.5X NBF and then transferred to 1x PBS until tissue processing. Additional details for all fixatives are listed in Table 1. The native biological tissue was processed as described previously using a xylene-free tissue processing routine (Silva et al., 2022). Prior to the embedding of the tissue, pieces were organized as "four spot" square tissue arrays into molten paraffin and allowed to cool as a single block. Paraffin-embedded tissue was cut into 5 µm tissue sections using a microtome (Model: 1516 Automated Leitz, Germany) and mounted on Super Frost adhesive microscope slides (Epredia, United States). Prior to chemical de-paraffinization, slides were placed vertically (lengthwise) overnight in a 65°C oven (ED56, Binder, Germany), followed by de-paraffinization using Histo-Clear (Ted Pella, United States).

Native tissue autofluorescence, staining and imaging

Prior to chemical-deparaffinization and rehydration, autofluorescence (λex = 469 nm, λem = 525 nm) was acquired using the manual imaging mode in a Cytation 5 multimode reader with a wide field camera (BioTek, Agilent Technologies, United States). Montage images were collected with the ×4 objective. GFP imaging filter cubes were used using the following acquisition settings for the liver, kidney, and heart: LED intensity: 2; integration time: 30 ms; camera gain: 24.

After de-paraffinization of TMA sections, microscopic slides were stained with hematoxylin and eosin (H&E) (Merck Millipore, Germany), dehydrated, and mounted with Pertex mounting media (Histolab, Sweden). Images were then captured with an inverted Nikon Ts-2R microscope using a 20X objective. Slide scanning was performed with the Cytation 5 multimode reader using the 4X objective and a wide field camera using the montage approach. With the selected area around the region of interest, the image was processed using the stitching tool image (linear blend)

TABLE 1 Overview of commercial and laboratory made fixatives used in this study.

Fixative name	Abb	Commercial product	Main fixation agent (%)	Ca^{2+} [mM]	Buffer (if known)	pH	Other known additives
Neutral-buffered formalin	NBF	Sigma	Formaldehyde (~3–5%)	0	30 mM NaH_2PO_4 46 mM Na_2HPO_4	7.4	Methanol (1%–3%)
		HT501128					
Formalin Free	FF	Sigma	Ethanol (30%–50%)	0	NA	3.9	*Proprietary, includes hydroxylated compounds*
		A5472					
Para-formaldehyde	PFA	Histolab	Formaldehyde from 4% PFA	0	100 mM PO_4^{3-}	7.4	-
		HL96753					
Glutaraldehyde	Glut	Sigma	2% Glutaraldehyde	0	37.7 mM PO_4^{3-}	7.3	PBS 18912014 Thermo Scientific, NBF
		G5882					
NBF with $CaCl_2$ addition	NBF_CA	Sigma	Formaldehyde (3%–5%)	50 mM	30 mM NaH_2PO_4 46 mM Na_2HPO_4	7.3	Methanol (1%–3%)
		HT501128					
PFA with $CaCl_2$ addition	PFA_CA	VWR	Formaldehyde from 4% PFA	1 mM	15 mM $Na_2HPO_4 \bullet 2H_2O$	7.4	DPBS (with 0.49 mM Mg^{2+})
		28,794.295					

parameter. Bright field color images of H&E-stained slides (i.e., following de-paraffinization and staining) were acquired at same time with identical settings using a 4X objective.

Cell culture

Human alveolar epithelial cells, A-549 (American Type Culture Collection, CCL-185, RRID:CVCL_0023) were cultured in Dulbecco's Modified Eagle Medium: Nutrient Mixture F12 (DMEM F12) (11554546, Fisher Scientific, Sweden) supplemented with 10% fetal bovine serum (FBS) (11573397, Fisher Scientific, Sweden), 1% penicillin and 1% streptomycin (15140122, Thermo Fisher Scientific) in a humidified incubator with air supplemented with 5.0% CO_2 at 37.0°C.

Inverted vial test

Stock solutions of 4% (w/v) alginate (Protanal-CR-8133, 9005-37-2 Pharma excipients) were freshly prepared in de-ionized water under constant agitation until all alginate dissolved and were allowed to rest until no air bubbles were visible. 2 mL of 4% sodium alginate solutions were mixed 1:1 (v/v) with phenol-containing DMEM/F12 to mimic tissue engineering and cell therapy approaches which encapsulate cells in alginate hydrogels. 750 µL of pre-gel solutions were added into 5 mL glass vials and crosslinked with 50 mM $CaCl_2$ (CAT. ID 21114-1L, Lot No. J3330) for 30 min to allow for hydrogel formation. 750 µL of $CaCl_2$ solutions were pipetted directly onto the center of the pre-gel solutions at the start and then slowly directed towards the sides. Prior to the addition of tissue fixatives, excess liquid which had not been incorporated into the hydrogel was removed, followed by the addition of the same fixatives used for native tissue and stored at room temperature NBF, FF, PFA, and Glut. For experiments evaluating the presence of hydrogel fragments in solutions, supernatant solutions were sampled at 1 and 24 h and placed on a microscopic slide for analysis using emboss contrast filters for three-dimensional appearing contrast of hydrogel fragments in an inverted Nikon Ts-2R microscope with a 10X objective. As controls, some calcium alginate hydrogels were incubated further in de-ionized water with and without 1 mM of $CaCl_2$ to stabilize the hydrogels (Kuo and Ma, 2008) and 25 mM ethylenediaminetetraacetic acid (EDTA) as a control for calcium chelation to induce dissolution of calcium alginate hydrogels into sodium alginate solutions. Vials were inverted and placed at a 45° inclination and images were taken at 1 h and after 24 h. Liquid was removed prior to all images after hydrogel formation to more readily allow for gel visualization.

UV-Vis spectroscopy of calcium alginate hydrogels in different fixatives

50 µL of sodium alginate, prepared as described for the inverted vial test, was pipetted into a 96 well microplate optimized for UV-Vis spectroscopy (82.1581.001, Sarstedt AB, Sweden). Ultraviolet-visible (UV-Vis) absorption spectra were then obtained for baseline samples in all wells from 330 to 700 nm wavelengths with a monochromator in 10 nm increments with the Cytation5 multimode reader (Biotek, Winooski, Vermont, United States). Sodium alginate solutions were then allowed to evaporate by incubtation at 65° C for at least 1 h until thin films were visible. Next, 50 µL of 50 mM $CaCl_2$ solutions were added to induce ionic crosslinking. After 30 min, $CaCl_2$ was removed and replaced with 100 µL of each fixative solution (n = 9 technical replicates). A breathable sealing tape with a hydrophobic surface on the sticky side (TMO241205, Sigma-Aldrich, United States) was then used to seal the microplate. De-ionized water with and without 1 mM $CaCl_2$ or with 25 mM EDTA was used as controls, similar to the inverted vial test. UV-Vis spectra were then acquired from 330 to 700 nm with 10 nm increments for pure fixative solutions and after 1 and 24 h of fixation, allowing for paired analysis of individual wells.

TABLE 2 Design of experiments (DOE) with two factorial design and four levels of each factor for a full factorial design. Factors were $CaCl_2$ crosslinking time (hours) and fixation time (hours). 50mM $CaCl_2$ crosslinking was performed for 0.5, 1, 2 h and overnight (18 h) while fixation time was 0, 1, 2 h and overnight (18 h). Each set of experiments was done in parallel for each fixative.

Experimental condition	$CaCl_2$ crosslinking time (hours)	Fixative time (hours)
1	18	1
2	2	2
3	2	0
4	1	18
5	2	1
6	0.5	18
7	1	1
8	0.5	1
9	1	0
10	2	18
11	1	2
12	18	18
13	18	0
14	0.5	0
15	0.5	2
16	18	2

Multifactorial design of experiments to determine crosslinking and fixation times suitable for each fixative

To determine conditions which could be suitable to later explore for assessing cell-containing constructs using histology, a multifactorial design of experiments (DOE) was conducted. As 50 mM calcium crosslinking is most commonly used for cell encapsulating manufacturing methods, such as 3D bioprinting, we set this as a control variable (i.e., constant). Through our previous experience, we have identified calcium crosslinking time, fixation time, and fixative as independent variables and maintenance of hydrogels as the most critical dependent variable to optimize for. Thus, a two-factor design of experiments with n = 4 levels (0, 1, 2, and 18 h) was established using the R Studio package "DoE.base" and the function fac. design with a seed = 4. Experiments were done using calcium alginate hydrogels manufactured using the diffusion through dialysis tubing approach, as described below, according to the DOE listed in Table 2 using technical triplicates.

Manufacture of calcium alginate hydrogels using diffusion through dialysis tubing

2% (w/v) solutions of alginate were placed in dialysis tubing (D9527-100FT, Sigma-Aldrich, Sweden) with a typical molecular weight cut-off = 12–14 kDa and completely submerged in 50 mM $CaCl_2$ in de-ionized water for 0.5, 1, 2, and 18 h. After each timepoint, crosslinked hydrogels were removed from the dialysis tubing and a 4 mm biopsy core was obtained and placed in a polystyrene Petri dish 60 × 15 mm (82.1194.500, Sarstedt AB, Sweden). An initial photo was collected using a Dino-Lite Edge Digital Microscope camera using the in-built DinoCapture Software V2.0 followed by addition of each fixative or 50 mM $CaCl_2$ as a control. Sequential images were acquired over time with each fixative. Images were blinded for semi-quantitative scoring with ordinal scoring of −1 (dissolved), 0 (deformed), 1 (preserved).

Contour maps were generated in R using the filled. contour function in the "ggplots" R package. Full code can be found on https://github.com/Lung-bioengineering-regeneration-lab/green_histology.

Manufacturing of hollow tubes containing cells using a 3D printed mold

A two-part polylactic acid (PLA, Eco White PLA 2.85 mm filaments, Dustin) mold was rendered using Shapr3D app for iPad and processed through Ultimaker Cura software prior to fabrication using a conventional extrusion 3D printer (Ultimaker 3, Creative Tools). Theoretical wall thickness between the inner and outer mold was 1 mm while molds with inner diameters of 6, 8, 10 mm were used in this study and a well-depth of approximately 5 mm .STL files are available at https://github.com/Lung-bioengineering-regeneration-lab/green_histology. Alginate (4% w/v) was diluted 1:1 in complete DMEM/F12 media containing 1 × 10^6 cells/mL. 50 mM $CaCl_2$ was first applied to the well and inserts of the 3D printed molds and aspirated off immediately prior to adding the alginate/cell solution. The inserts of the 3D printed molds were placed into the center of each well and the alginate/cell solution was slowly applied until the entire tube portion of the well was filled. Then, 50 mM $CaCl_2$ was applied on top of all tubes, filling the upper chamber of the molds (i.e., solution reservoir). After 30 min, the excess $CaCl_2$ was removed and the inner portion of the mold was removed. Tubes were carefully removed from the insert and moved to a 24-well plate. Some tubes were immediately processed for fixation while others were covered with 2 mL complete media and cultured overnight and fixed on the following day with either FF or PFA_Ca. The tubes cultured overnight and fixed both with FF or PFA_Ca were subjected to tissue processing and histologically processed for blinded scoring as described below.

Manufacture of alginate and alginate-gelatin films

Alginate and alginate-gelatin thin films were fabricated *via* casting. 4 mL of either 2% (w/v) alginate or 2% (w/v) alginate with 5 mg/mL of gelatin (410875000, Acros, Fisher Scientific) were poured into 60 mm diameter polystyrene Petri dishes (Sarstedt) and placed into an oven at 65 °C (ED56, Binder) for at least 2 h until all liquid had evaporated. Films were then carefully removed from the Petri dish and subsequently manufactured into discs with an 8 mm diameter biopsy punch. Dry disks were then weighed using a precision scale (Mettler Toledo) and their radius

was measured optically using a DinoLite camera and the in-built three-point circle function in the DinoCapture software version 2.0 to calculate the radius. Next, disks were rehydrated and crosslinked using 50, 200 or 500 mM of $CaCl_2$ solution for 1 h followed by incubation overnight (i.e., 18 h) with complete cell culture and finally fixation in either PFA_Ca or FF. Mass swelling ratios were calculated according to the following formula:

$$swelling\ ratio\ (\%) = \frac{crosslinked\ weight\ (g) - dry\ film\ weight\ (g)}{dry\ film\ weight\ (g)} \times 100\% \quad (1)$$

Cell culture on alginate or alginate-gelatin films for cross-sectional histology

Thin films were manufactured as above using 200 mM of $CaCl_2$ crosslinking. Prior to cell seeding, calcium alginate membranes were placed into the center of a 24-well tissue culture plate (83.3922, Sarstedt AB, Sweden) and allowed to dry. 100,000 cells suspended in 25 µL of media were placed as a single droplet onto the center of each disk and allowed to attach in the incubator for 30 min. Next, 500 µL of media was slowly added to each well and disks were cultured for 36 h prior to fixation or metabolic assessment. At the completion of cell culture, disks were imaged using embossed contrast (EC2) with a 20X objective on a Nikon Ts-2R inverted microscope followed by fixation in FF or PFA_Ca using the same method as described above for tubes. Samples for histological processing were stored in 70% ethanol in 24-well plates until placing in a tissue processor or proceeding to processing for scanning electron microscopy as described below. All experiments were done at least three times (N = 3) with at least n = 4 technical replicates.

Fixation of 3D tissue engineered tubes and membranes for tissue processing

Media was carefully removed followed by the addition of 5 mL of either FF or PFA_Ca fixative directly into the well for 30 min. Tissue processing commenced thereafter by performing the first dehydration step in 70% ethanol in the well and then carefully placing the tubes into cassettes with foam pads to stabilize them during tissue processing. Cassettes were then loaded into an automatic tissue processor (Automated Spin Tissue Processor, model: STP 120, Myr) in an ascending series of ethanol solutions 70% and 80% ethanol, 2% × 80% ethanol and 20% isopropanol, followed by 3% × 100% 2-propanol (15,518,744, Fisher Scientific, Sweden). Each step was 1 h long and was conducted without stirring. Initial paraffin infiltration occurred for 3 h and was followed by a second incubation in paraffin for at least 6 h (Histowax (00403), Histolab, Sweden). Tubes were oriented in paraffin with the lumen parallel to the cutting surface. Membranes were oriented in paraffin blocks with their cross section parallel to the cutting surface. This was accomplished by first cutting paraffin infiltrated membranes in half with a scalpel. Next, membranes were dipped into molten paraffin to increase their thickness to allow for orienting in the metal molds prior to filling with liquid paraffin. Paraffin blocks were allowed to cool and then 5 µm thick slices were generated with a microtome and placed on Super Frost Microscopic Slides and allowed to dry prior to staining. Staining was performed as previously described, but with reduced hematoxylin staining of 5 min due to the large uptake of hematoxylin in alginate hydrogels we observed in pilot experiments.

Cell counting

Calcium alginate tubes containing cells were either fixed with PFA_Ca or FF and subjected to xylene free histological processing, paraffin embedding and sectioning for H&E staining. 20 random brightfield pictures from were taken from transverse histological sections of tubes with a 10X objective using an inverted Nikon TS-2R microscope. Images were then blindly scored by an independent observer who had not previously seen the images and quantified using the ImageJ tool "Cell counter". The number of normal appearing cells per field, cells with visible separation from the biomaterial and empty spaces were quantified. Next, the total number of cells was calculated by adding the number of normal cells and cells exhibiting detachment from the biomaterial. The percentage of cells exhibiting detachment from the biomaterial to the total number of cells present in the field was then calculated.

Water-soluble tetrazolium-1 viability assay (WST-1)

Water-soluble tetrazolium salt reagent (WST-1) was used to assess metabolic activity of tissue engineered constructs. Crosslinked calcium alginate and calcium alginate-gelatin films seeded with cells, as described above, were incubated with 1 mL of complete cell culture medium and 100 µL WST-1 (Roche, Sigma-Aldrich, United States) for 1 h in a humidified incubator with 5% CO_2 in air at 37°C. Then 3 replicates of 100 µL of the supernatants from each well were removed and pipetted into a new 96 well plate. Optical density was measured at 440 and 650 nm (Epoch plate reader, BioTek, Winooski, Vermont, United States). Cell free calcium alginate and cell free calcium alginate-gelatin films manufactured and cultured in parallel served as negative controls. Absorbance at 650 nm was subtracted from all 440 nm absorptions to account for non-specific absorbance.

Scanning electron microscopy (SEM)

For SEM preparation, calcium crosslinked hydrogel disks were fixed in FF or PFA_Ca for 30 min, then dehydrated in serial solutions of 80% and 90% ethanol in de-ionized water, for 3 minutes each, and followed by 100% ethanol for 3 × 3 min for each dehydration step. The samples were then stored in 100% ethanol until chemical dehydration treatment with hexamethyldisilazane (HMDS, Ted Pella, United States) in serial grading 33%, 50%, and 66% HMDS in ethanol for 5 min each, followed by 100% HMDS for 5 min. The samples were then left to dry in a chemical fume hood for 30 min, then fixed on SEM stubs with a conductive silver paint (Ted Pella, United States) and were

sputter coated with platinum-palladium at 80:20 ratio (Q150T ES, Quorum Technologies, United Kingdom) at 10 nm thickness with 40 mA sputter current before being mounted and examined in a Jeol JSM-7800F FEG-SEM under secondary electron imaging mode at 3.0 kV accelerating voltage.

Power and statistical analysis

Statistical analyses were performed using GraphPad Prism 9 unless otherwise stated. Owing to the low sample numbers as well as variability in manual measurements and manufacturing approaches utilized here, all measured populations were assumed to have non-parametric distributions. The statistical test used and central tendency measures used are listed in the corresponding figure legends. Power analyses to determine the number of n's needed for determining the swelling ratio and change in dimensions for cast films was done using pilot data. Power analyses were conducted in R using the "pwr2" package.

Results

Commercial and laboratory made fixatives comparably preserve histological architecture of diverse native tissue types

Alginate hydrogels are currently being investigated for a range of different clinical scenarios which span multiple organs and tissue types. As different types of fixatives preserve cellular and tissue level structures using different underlying chemical principles (i.e., chemical crosslinking of specific amino acid residues *versus* coagulation/denaturing) (Werner et al., 2000; Howat and Wilson, 2014), we first aimed to test the potential of four different commercially available fixatives in preserving native tissue architecture across organs with differing biological composition (e.g., lipid *versus* protein ratio) (Schoephoerster et al., 1985; Jain et al., 2014). Among fixatives which fix tissue *via* covalent crosslinking, we selected 10% NBF containing methanol to stabilize formaldehyde and prevent its degradation or precipitation, 4% PFA in 0.1 M phosphate buffer, and 2.0% electron microscopy grade glutaraldehyde in PBS. For coagulation-based fixation, we used a commercially available fixative which is environmentally sustainable and FF, Accustain (Sigma). Accustain is a proprietary formulation but is known to contain ethanol and its pH is acidic. Table 1 provides an overview of all fixatives used in this study.

In order to remove any potential bias due to changes in tissue thickness between biopsy pieces randomly allocated to the different fixatives, we first generated precision cut tissue slices using a vibratome (275 µm for brain and 200 µm for heart, liver, and kidney) and fixed parallel slices of each organ in one of the four commercially available fixatives overnight to mimic standard pathological fixation protocols. Next, we simultaneously processed all tissue pieces using a modification of a xylene-free tissue processing protocol we recently described for large animal organs which uses isopropanol instead of xylene for removal of ethanol to clear tissues and permit paraffin infiltration (Silva et al., 2022). We then created tissue specific tissue microarrays (TMA) containing one tissue slice fixed for each of the four different fixatives. Next, we generated individual paraffin sections of the TMAs to allow for simultaneous staining of tissue pieces to allow direct comparison (Supplementary Figure S1). As (immuno)fluorescence-based imaging is often used to evaluate tissue engineered constructs, including after implantation, we analyzed changes in tissue autofluorescence with each of the different fixatives and the xylene free tissue processing protocol for liver, kidney and heart prior to de-paraffinization. Similar to previous studies, we found that glutaraldehyde based fixation resulted in increased tissue auto-fluorescence (Supplementary Figure S1A) (Lee et al., 2013). In addition, we found that all four fixatives were able to comparably retain tissue architecture but that the degree of H&E staining differed depending on the fixative, with glutaraldehyde and NBF showing weaker eosin staining (Figure 1) as previously observed in studies comparing aldehyde based crosslinking to alcohol based fixatives (Perry et al., 2016). Taken together, this indicates that all four of the chosen commercial fixatives can be used in combination with xylene-free tissue processing protocols and could potentially be used to histologically evaluate alginate-based scaffolds.

Ethanol based, formalin-free fixative preserves hydrogel structure during standard fixation times

Despite the fact that these fixatives appeared to perform somewhat comparably for fixation of native tissues, fixation of ionically crosslinked calcium alginate is known to be challenging (McGowan and Nagatomi, 2013). In order to evaluate the potential of these 4 commercially available fixatives, we established conditions to mimic *in vitro* calcium alginate hydrogel formation for cellular encapsulation or generation of cell-laden hydrogels. We prepared 2% (w/v) sodium alginate in DMEM/F12 cell culture media (containing 1 mM Ca^{+2}). Then, we carefully cross-linked sodium alginate with an equal volume of 50 mM $CaCl_2$ and allowed ionic crosslinking to occur over 30 min (Figure 2A). After obtaining calcium alginate hydrogels, we added one of the 4 different commercially available fixatives (NBF, FF, PFA and Glut) and compared these to three control solutions: H_2O, H_2O containing 1 mM $CaCl_2$, and H_2O containing 25 mM EDTA. After 1 h of fixation, we observed that hydrogels incubated in NBF, FF and Glut were macroscopically preserved, but incubation of calcium alginate hydrogels in PFA resulted in loss of the bulk hydrogel (Figure 2B). As expected, incubation in 25 mM EDTA resulted in complete dissolution of gels at the same time point, while calcium alginate hydrogels incubated in H_2O and H_2O supplemented with 1 mM $CaCl_2$ were retained at 1 h (Supplementary Figure S2A). After 24 h of fixation, which mimics many recommended protocols for formaldehyde-based crosslinking, we observed that bulk hydrogels were no longer visible in all fixatives except the Glut and FF, while they were retained in H_2O controls (Figure 2B, Supplementary Figure S2A). FF appeared to keep the entire calcium alginate hydrogel intact, while Glut only was able to retain a thin hydrogel after 24 h fixation, indicating significant loss of the bulk hydrogel in comparison to the hydrogel present after 1 h of fixation.

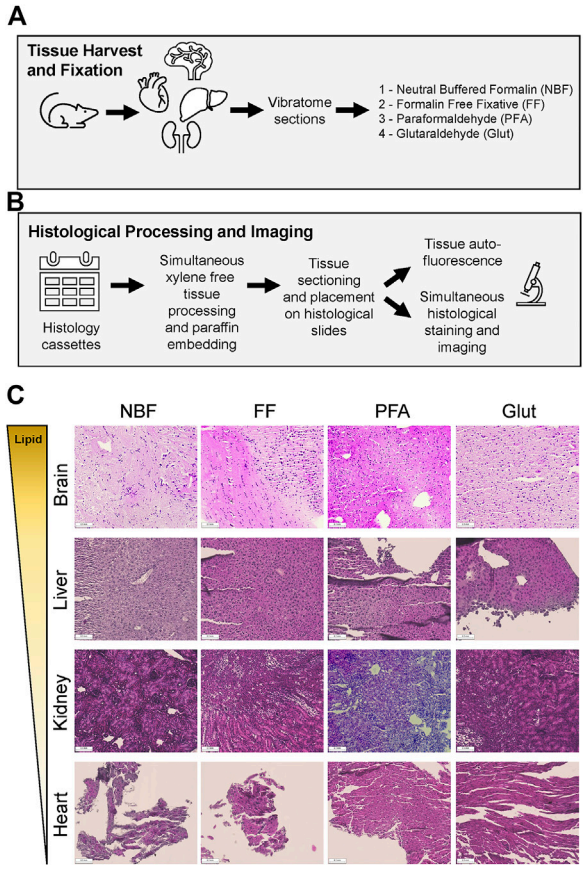

FIGURE 1
Fixation of native murine tissues of varying lipid-protein composition with different commercially available fixatives. **(A)** Overview of tissue harvest (brain, heart, kidney and liver) from a single animal followed by vibratome slicing and then fixation of neighboring sections using one of four commercially available fixatives (detailed in Table 1). **(B)** Overview of histological processing workflow to generate tissue microarrays (TMAs) for assessing tissue autofluorescence with different fixatives and simultaneous staining with hematoxylin and eosin (H&E) and imaging. **(C)** Organs are arranged from highest to lowest lipid content. H&E images acquired using a ×20 objective on a Nikon Ts-2R inverted microscope with constant acquisition settings for all images. Scale bar is 100 μm for all images. Schematic in **(A)** and **(B)** made using Microsoft Icons by the authors.

In order to gain further insight into these changes, we collected UV-Vis absorption spectra in parallel to examine whether fixatives caused true dissolution to sodium alginate precursor solutions or rather that the fixatives resulted in dissociation of bulk hydrogel networks while managing to induce some degree of smaller, chemically crosslinked gel fragments (i.e., colloidal solution of chemically crosslinked gels). While aldehyde based crosslinking is known to mainly occur through imine formation on lysine residues in native tissues (Tayri-Wilk et al., 2020), crosslinking of alginate hydrogels by aldehydes has previously been reported to be due to crosslinking between hydroxyl groups present in alginate (Yeom and Lee, 1998). While both formaldehyde and glutaraldehyde can theoretically impart these crosslinks, formaldehyde is smaller and can thus penetrate tissues and hydrogels more quickly. However, the kinetics of formaldehyde based crosslinking is slower and thus longer incubation times are often needed (Kiernan, 2000). We observed that the buffering solutions used for the different aldehyde based crosslinking fixatives (i.e., corresponding buffer composition without fixatives) were able to dissociate the bulk hydrogels into smaller hydrogel fragments as early as 1 h (Supplementary Figure S3). Thus, in calcium alginate-based hydrogels, aldehyde induced crosslinks must chemically stabilize the hydrogel faster than calcium is released from the hydrogel, due to the buffer conditions, to keep the entire tissue construct intact during the entire fixation time.

Therefore, we monitored kinetic changes in UV-Vis absorption spectra across all experimental time points (ionic calcium crosslinking to induce hydrogel formation, 1 h after fixation and 24 h after fixation). As expected, we observed increases in absorption after ionic crosslinking of sodium alginate to calcium alginate in all experimental groups (Figure 2C, Supplementary Figure S2C), indicating successful formation of a hydrogel with significantly altered optical properties [i.e., area under the curve (AUC)] as compared to the starting sodium alginate solution or $CaCl_2$ solution alone (Figure 2D, Supplementary Figure S2D). In addition, we observed the presence of the characteristic phenol peak at ~560 nm in both sodium alginate and calcium alginate due to the use of phenol containing medium in these experiments to mimic typical cell culture conditions. After applying fixatives for 1 h, we noticed that UV-Vis spectra remained the same or elevated for all fixatives (i.e., NBF, FF, PFA, and Glut) despite the fact that some of these solutions caused visible dissolution of bulk hydrogels (Figure 2B, Supplementary Figure S3B). However, incubation in aldehyde-containing fixatives induced further significant increases of AUC at 24 h (Figure 2D), likely due to further changes in the hydrogel structure, such as chemical crosslinking (Supplementary Figure S3B) Interestingly, we did not observe any changes with time for formalin-free fixation, indicating that fixation was rapid and that the hydrogel structure did not further change over time (Figures 2C, D, Supplementary Table S1).

Ethanol based, formalin-free fixative and calcium containing fixatives preserve hydrogel structure during standard fixation times

As a variety of different manufacturing methods for generating ionically crosslinked calcium alginate hydrogels are available, we next sought to determine if there was a relationship between calcium crosslinking time, type of fixative and fixation time on the stability of calcium alginate hydrogels. In addition, we sought to better understand the impact of different additives and minor components of the commercially available fixatives we previously evaluated in native tissues (Figure 1). Therefore, we additionally explored the potential of NBF with added calcium chloride (50 mM Ca^{2+}) as well as freshly made laboratory PFA in Dulbecco's phosphate buffered saline (D-PBS) containing 1 mM Ca^{2+} and 0.5 mM Mg^{2+} (Table 1), divalent cations which have been shown to help stabilize calcium alginate hydrogels at these concentrations during *in vitro* culture (Kuo and Ma, 2008). We first established a design of experiments using a two-factor design to cover commonly used laboratory time intervals of the manufacturing and fixation process which were viewed as independent variables (Table 2). As a process readout, we aimed to utilize blinded scoring of calcium

10.3389/fbiom.2023.1155919

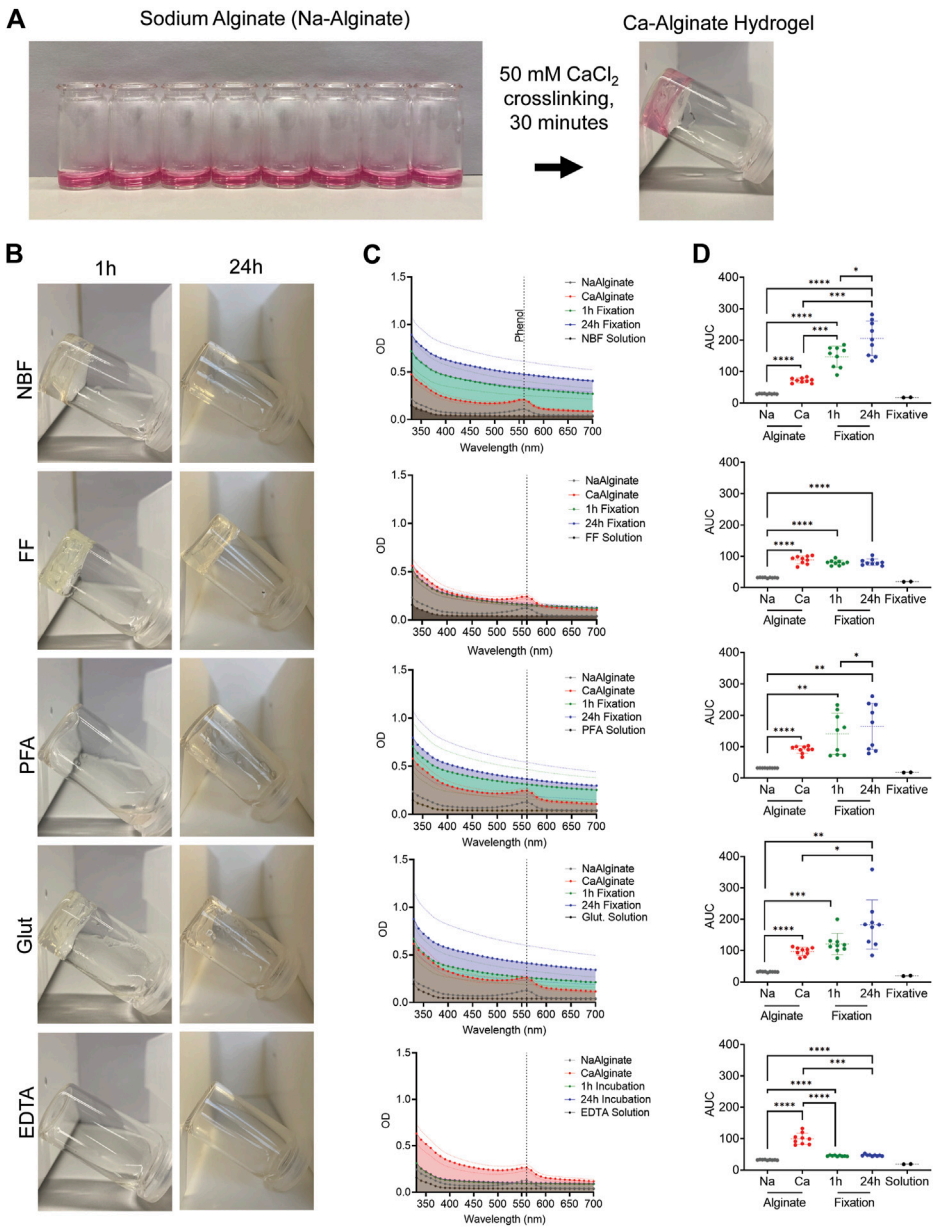

FIGURE 2
Fixation of calcium alginate hydrogels with different commercial fixatives for inverted vial test and UV-Vis Spectroscopy. **(A)** Crosslinking of sodium alginate in DMEM/F12 media to calcium alginate was performed in 5 mL glass vials using $CaCl_2$ to form hydrogels. **(B)** Representative photomicrographs of hydrogels, with liquid removed, at an inclination of 45° after 1 and 24 h fixation in commercially available fixatives: neutral-buffered formalin (NBF), formalin free fixative (FF), paraformaldehyde in 0.1M phosphate buffer (PFA), glutaraldehyde (Glut) and 25 mM EDTA as dissolution control. **(C)** UV-Vis absorption spectra across all experimental time points: sodium alginate (gray), calcium alginate (red), 1 h fixation (green), 24 h fixation (blue) and pure fixative solution (black). **(D)** Area under the curve (AUC) calculated per condition, the same color code is used as for UV-Vis absorption spectra. Statistical analysis for all fixatives was evaluated using a repeated measure two-way ANOVA comparing changes in AUC across all experimental conditions and fixatives. Repeated measures with Geisser-Greenhouse correction and Tukey's multiple comparisons test with individual variances computed for each comparison. Complete overview given in Supplementary Figure S2D. * indicates statistical significance; *p*-values <0.05 considered statistically significant. * indicates *p*-values considered statistically significant: *$p < 0.05$, **$p < 0.005$, ***$p < 0.0005$, and ****$p < 0.0001$.

alginate hydrogels from serial photographs with three levels of scores (−1, 0, and +1 corresponding to dissolution of the hydrogel, distortion of the hydrogel, and preservation of the hydrogel).

In our previous experiments, calcium crosslinking occurred isotropically *via* a diffusion gradient within the glass vial (i.e., from top to bottom). While this setup is ideal for conducting the inverted vial test to assess transitions between solutions and hydrogels (as well as their dissolution or disintegration), the initial exposure to calcium is known to rapidly create a hydrogel network at the interface, which then slows the diffusion of calcium further into the alginate solution to complete crosslinking (Julian et al., 1988). Furthermore, this gelation method does not mimic many calcium crosslinking

procedures used to generate ionically crosslinked alginate hydrogels. In most current manufacturing techniques for tissue engineering and cell therapy approaches, alginate pre-gel solutions are exposed to spatially homogenous reservoirs of calcium ions through external or internal gelation approaches to generate more stable hydrogels. Such gelation processes occur during many types of extrusion-based 3D bioprinting with alginate as well as during cellular encapsulation-based approaches. Thus, we used a diffusion through dialysis tubing approach (Bajpai et al., 2017) to simulate these types of manufacturing approaches and exposed sodium alginate solutions to different amounts of calcium crosslinking times prior to exposing them to each of the different fixatives and fixation times. We found that there was a clear relationship between calcium crosslinking time and hydrogel stability following fixation time. In general, increased time of calcium chloride exposure led to the formation of hydrogels which could withstand longer fixation times (Figure 3). However, fixatives which stabilize tissue *via* chemical crosslinks and contained no added calcium ions and high amounts of phosphate (i.e., NBF and PFA) caused physical disintegration of the gels upon macroscopic observation, as we observed previously in calcium alginate hydrogels formed from one-dimensional calcium gradients (Figure 2).

Ethanol based, formalin-free fixation preserves calcium alginate-cell interactions in 3D cast tubes and allows for histological processing using xylene free approaches

Having identified process relationships between calcium crosslinking time, fixative type and fixative time, we next sought to evaluate the feasibility of these fixation approaches to histologically assess 3D calcium alginate scaffolds containing cells. We used two-part 3D printed polylactic acid (PLA) molds (Figure 4A) to fabricate calcium alginate tubes containing encapsulated cells followed by fixation in either FF or PFA_Ca. We selected these two fixatives as we found that only FF, Glut, and PFA_Ca preserved macroscopic hydrogel architecture under conditions of short crosslinking times (Figure 3). It has been previously shown that both the concentration of calcium and the time of exposure impacts cellular viability. Most studies indicate that Ca^{2+} concentrations below 100 mM and for less than 30 min are suitable for calcium crosslinking of low weight percentage sodium alginate solutions (Cao et al., 2012; De Santis et al., 2021). Higher concentrations of calcium (>200 mM) have also been successfully used with good viability if shorter crosslinking times are used. However, this is only feasible for manufacturing approaches with micrometer sized dimensions (e.g., cellular encapsulation in microspheres). Larger constructs, such as those fabricated with 3D bioprinting, may be exposed to increased calcium concentrations for >1 h with larger prints. Therefore, we opted to use 50 mM of $CaCl_2$ for all experiments where live cells were to be incorporated into final constructs (Figure 4B).

We found that calcium alginate tubes could be fabricated using this method, although the walls of the tube were thin and thus they needed to be removed from the molds with care. Nonetheless, 3D calcium alginate tubes were then cultured in standard complete media which contains around 1 mM of Ca. We observed noticeable increases in the size of the tube with culture time using this method (*data not shown*) and the tubes became more difficult to handle after longer culture times, as has previously been described for calcium concentrations below 1 mM (Kuo and Ma, 2008). Therefore, for our proof-of-concept studies, we opted to perform FF or PFA_Ca crosslinking after only 12 h of culture time. We found that both PFA_Ca and FF macroscopically retained the structure of the calcium alginate tubes containing cells, but that the PFA_Ca tubes were more difficult to handle. Therefore, after fixation in the tissue culture wells with PFA_Ca or FF, we performed the initial dehydration step of 70% ethanol in the tissue culture wells which we found helped in handling the tissue engineered constructs. Following dehydration in 70% ethanol, calcium alginate hydrogels were transferred to histological cassettes for xylene-free tissue processing followed by routine H&E staining (Figures 4C, D). In order to assess differences between FF and PFA_Ca crosslinking, we performed blinded scoring of presumed tissue artefacts such as separation between the calcium alginate hydrogel and cells which has also been observed in previous studies utilizing formalin with added calcium (Khatab et al., 2020). We found that tubes fixed with PFA_Ca had a significantly increased percentage of separation artefacts as well as a significantly increased number of empty histological regions without cells (Figures 4E–G). This may be due to the swelling which occurs upon exposure to PO_4^{3-} ions which can result in loss of calcium from the hydrogel and thus relaxation of the ionically crosslinked alginate hydrogel network allowing for water uptake before chemical fixation occurs (Segale et al., 2016). Altogether, this demonstrates that FF preserves both the macroscopic and microscopic structure of cell-biomaterial interactions in calcium alginate hydrogel scaffolds and permits histological processing with less artefacts.

Ethanol based, formalin-free fixation permits histological evaluation of thin alginate and alginate-gelatin constructs for histological and SEM visualization of epithelial monolayers

Despite alginate's widespread usage as a tissue engineering scaffold, it is highly hydrophilic and does not contain native binding sites for cells (Rowley et al., 1999). Therefore, in order for cells to be seeded on top of calcium alginate hydrogels, one of several modifications needs to occur. One option is the adsorption or covalent attachment of ECM proteins on the surface of the alginate hydrogel (e.g., collagen type I) (Gepp et al., 2017; Neves et al., 2020). Alternatively, ECM proteins such as gelatin or decellularized ECM can be incorporated directly by mixing them with alginate. Their inclusion has recently been shown to reduce swelling of calcium alginate-based hydrogels allowing for longer term and more stable culture (De Santis et al., 2021; Temirel et al., 2022). In order to evaluate whether FF could work in hybrid alginate systems, we fabricated sodium alginate or sodium alginate-gelatin films of 8 mm diameter followed by crosslinking with 50, 200 or 500 mM $CaCl_2$

10.3389/fbiom.2023.1155919

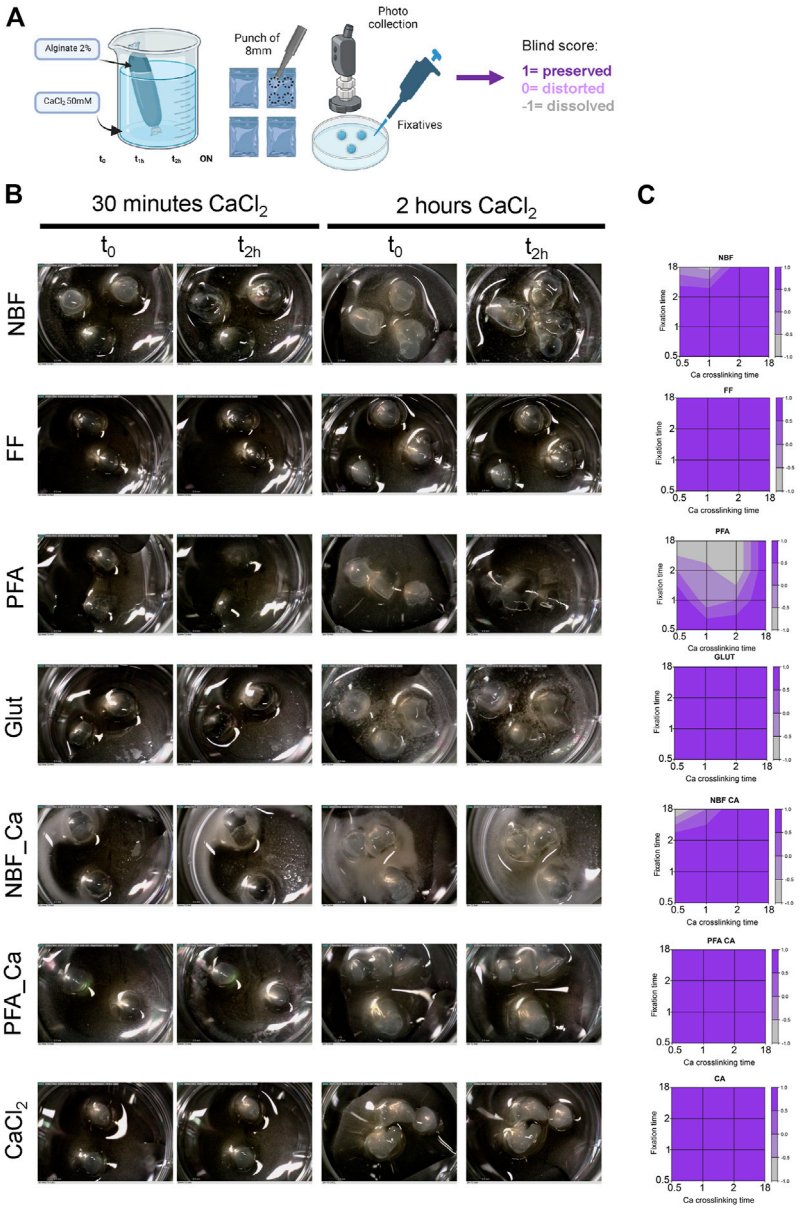

FIGURE 3
Results of design of experiments evaluating the relationship between calcium crosslinking time, fixative and fixation time. **(A)** Experimental overview for generating crosslinked calcium alginate based hydrogels *via* diffusion in dialysis tubing followed by fixation and blinded scoring. **(B)** Representative image for 30 min and 2 h of calcium crosslinking time and immediately after fixation and after 2 h of fixation for various fixatives as listed. **(C)** Contour plots of blinded scoring. Figure 3A made using Biorender.

solutions to create thin membranes (Li et al., 2016). In line with our use of 50 mM in the previously manufactured calcium alginate hydrogels, we first evaluated the feasibility of using 50 mM crosslinking of these thin sodium alginate films for use as cell culture supports of epithelial monolayers. We found that there was no statistically significant change in the radius of crosslinked calcium alginate hydrogels as compared to dry films, but that the radius of the calcium alginate hydrogels significantly increased by ~36% after incubation with DMEM/F12 (4.25 ± 0.07 mm for crosslinked *versus* 5.77 ± 0.29 mm for calcium alginate hydrogels incubated with cell culture media) (Supplementary Figure S4A) mimicking *in vitro* cell culture conditions with <1 mM of calcium ions (Kuo and Ma, 2008). However, we found that calcium alginate hydrogels crosslinked with 50 mM of $CaCl_2$ could not be processed further with either FF or PFA_Ca as they were destroyed during handling prior to fixation. Therefore, we next evaluated the potential of 200 or 500 mM $CaCl_2$ crosslinking on sodium alginate and sodium alginate films to fabricate thin hydrogel membranes. We found that the swelling ratio was unchanged when comparing 200 *versus* 500 mM $CaCl_2$ crosslinking (Supplementary Figure S4B). Furthermore, we observed statistically significant decreases in the crosslinked hydrogel radius as compared to the dry film radius

10.3389/fbiom.2023.1155919

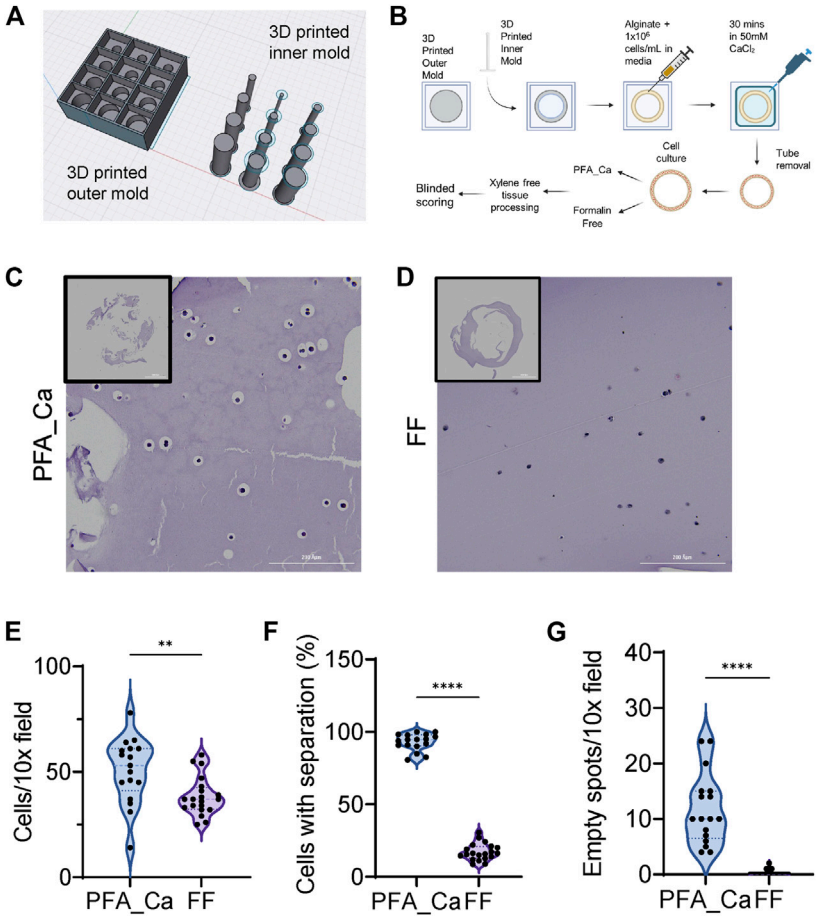

FIGURE 4
Fabrication of 3D alginate tubes containing cells using a two-part 3D printed PLA mold. **(A)** 3D printed mold for constructing calcium alginate tubes constructed in Sahpr3D. **(B)** 3D printed inner molds are placed inside the outer mold and lightly dipped in 50 mM calcium chloride solution. The inner portion of the mold is slowly filled with sodium alginate and cell solutions until it reaches the top of the depressed region of the mold. Next 50 mM calcium chloride solution is placed on the crosslinking reservoir above the tube and sodium alginate solutions containing cells are allowed to crosslink for 30 min. Tubes are then carefully removed and subjected to cell culture overnight followed by fixation in PFA_Ca or FF and processed using a xylene free tissue processing routine. H&E sections were then blindly scored. **(C)** PFA_Ca and **(D)** FF fixed calcium alginate tubes. **(E)** Number of cells per field captures with a 10X objective shows a significant reduction in the number of cells detected per field with FF. **(F)** Percentage of cells with separation between cell and biomaterial. **(G)** Number of empty spots per field of view captured with a 10X objective shows a significantly increased number of empty spots in PFA_CA as compared to FF. Central tendency measures on violin plots: long dashed lines is the median while shorter dashed lines indicated quartiles. * indicates p-value<0.05. All statistical analyses were performed using Mann-Whitney Rank Test due to the non-normality of the data. Experiments are representative of two independent experiments (N = 2) with at least three technical replicates each time (n = 3). Figure 4B made with Biorender.

for all compositions (Supplementary Figure S4C). Therefore, we opted to proceed with sodium alginate and sodium alginate gelatin films crosslinked with 200 mM to minimize the amount of calcium which might leach into the cell culture medium during cell culture, potentially effecting cell behavior.

Next, we seeded immortalized human lung epithelial cells on the apical surface of calcium alginate and calcium alginate gelatin membranes fabricated with 200 mM $CaCl_2$ and allowed them to grow under standard cell culture conditions for 36 h (Figure 5A). As expected due to the fact that alginate alone contains no binding sites for cell adhesion (Rowley et al., 1999), we found that cells seeded onto the alginate only scaffolds were only lightly adherent to the scaffolds, while alginate-gelatin hybrid scaffolds contained more cells and with subjectively more cells displaying a flattened or adherent morphology (Figure 5B). These microscopic observations correlated with statistically significant increases in metabolic activity between alginate and alginate-gelatin scaffolds according to metabolic assessment with WST-1 (Figure 5C).

Next, we sought to confirm whether FF could be used to generate thin cross sections of the membranes using histological approaches. Fixatives causing dissolution or disintegration of ionically crosslinked calcium alginate hydrogels would make thin membranes difficult to process and section. We found that FF preserved the morphology of the membranes and that similar to live imaging, histological cross sections showed that FF could be used to preserve cell-biomaterial interactions of cells growing on the alginate-gelatin membranes (Figure 5B). On the other hand,

10.3389/fbiom.2023.1155919

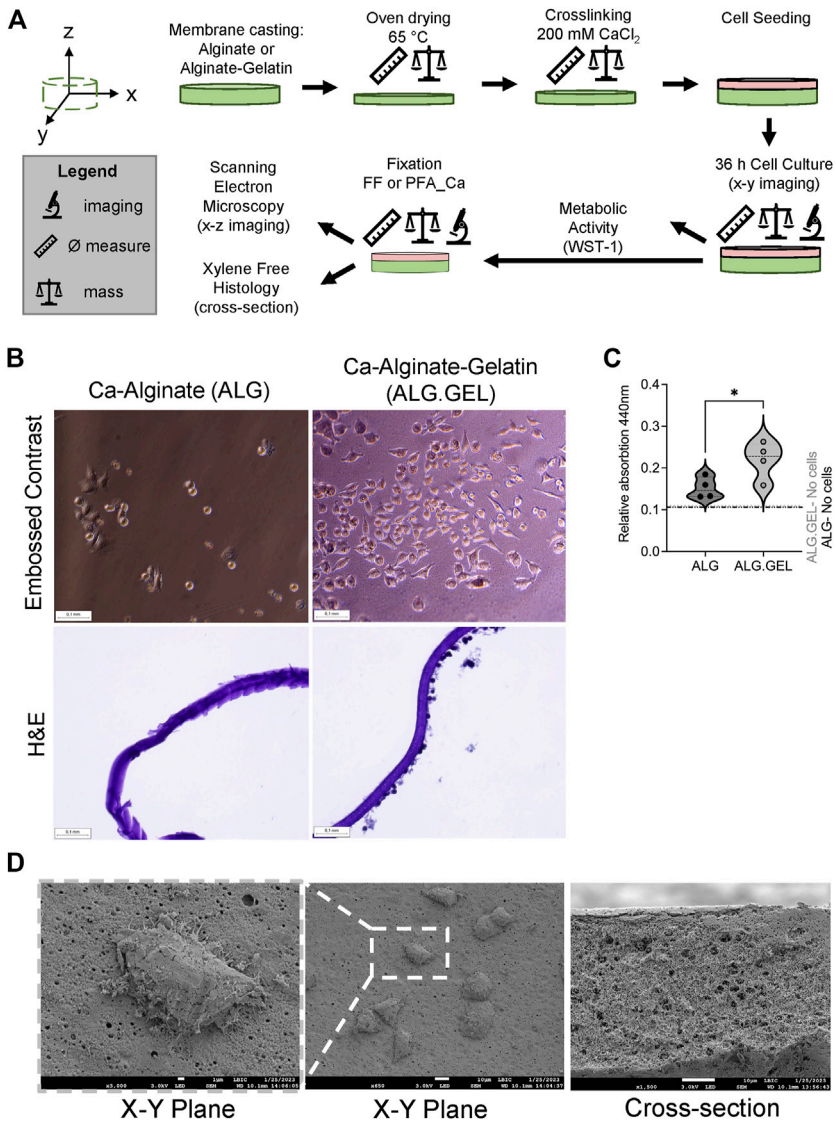

FIGURE 5
Fabrication and characterization of epithelial cells grown on alginate and hybrid alginate-gelatin membranes for histological cross section and scanning electron microscopy evaluation. **(A)** Schematic overview of the manufacturing process as well as data collection. **(B)** Embossed contrast imaging (representing x-y) imaging of cells grown on alginate *versus* hybrid alginate-gelatin membranes. H&E cross sectional (x−z) plane imaging showing monolayers of epithelial cells growing on only one side of a membrane. Both membranes were processed using FF fixation. **(C)** Increased metabolic activity as assessed by WST-1 assay. Individual dots are technical replicates (n = 4) from the same manufacturing and cell seeding experiment. Representative of 3 independent experiments (N = 3). Calcium alginate and hybrid calcium alginate-gelatin membranes without cells but cultured under identical conditions serve as controls. All WST-1 values are above background levels. **p*-value<0.05 is considered statistically significant. Non-parametric, Mann-Whitney *t*-test. Central tendency data is shown with a darker dashed line to indicate the median while lighter dashed lines indicate quartiles. **(D)** SEM micrographs of the apical and cross sectional surface of a hybrid alginate-gelatin membrane fixed using FF and chemically dried with HMDS. Retention of fine structures, such as individual lamellipodia are still visible, demonstrating cell-biomaterial interactions. Cross sectional view of hybrid alginate-gelatin membrane demonstrating retention of porous structure during preparation from fixed FF samples. Schematic in Figure 5A made using Microsoft Icons.

membranes fixed with PFA_Ca were unable to be processed and were found to be too delicate to handle for histologically processing (*data not shown*).

Finally, having confirmed that FF could be used to preserve cell-biomaterial interactions on hybrid alginate-gelatin thin membranes, we sought to explore whether FF could be used as a substitute for glutaraldehyde-based chemical fixation, which is known to be state-of-the-art for preparing samples for electron microscopy. Similar to a previous report which demonstrated that FF could be used to preserve cellular morphology for SEM analysis on collagen coated polydimethylsiloxane (PDMS) substrates (Bettinger et al., 2008), we found that FF and chemical drying with HMDS preserved cell-biomaterial interactions and additionally preserved hydrogel architecture which was subjectively comparable to morphologies observed in previous studies with cryo-SEM approaches (Koch and Włodarczyk-Biegun, 2020) (Figure 5D). Taken together, FF fixation

is a promising alternative to aldehyde based chemical fixation which results in artefacts. FF fixation permits histological and SEM evaluation of ionically crosslinked calcium alginate and hybrid calcium alginate-gelatin scaffolds during multiple stages of manufacturing and cell culture.

Discussion and conclusion

While buffered and osmotically balanced solutions are required for chemical fixation of native tissues, the type of buffer and additional additives, even at low concentrations, can dramatically impact the stability of ionically crosslinked hydrogels over time. In particular, most commercially available fixatives use phosphate as the buffering agent. Calcium and phosphate are known to rapidly precipitate into insoluble amorphous precipitates due to the low solubility of calcium phosphates at physiologic pH (Dorozhkin, 2016). Formation of $Ca_xH_y(PO_4)_z$ nH_2O precipitates, even if amorphous (Wagner et al., 2013), will thus lower the amount of calcium available to support the stability of ionically crosslinked hydrogels during chemical fixation. Furthermore, we experimentally observed that the phosphate concentrations present in the commercially available buffers were sufficient to dissociate ionically crosslinked calcium alginate hydrogels at the bulk hydrogel level, but small hydrogel fragments could still be observed microscopically after incubation in the buffer solutions (Supplementary Figure S3). Our UV-Vis spectroscopy-based experiments (Figures 2B,C) confirmed this finding and we did not observe any noticeable reduction in absorbance for PFA or NBF. This indicates that the macroscopically visible dissolution resulted in the formation of a colloid solution (Argenta et al., 2019) instead of complete dissolution into sodium alginate solution, as was observed with EDTA controls (Figures 2B,C, Supplementary Figure S3). Therefore, it is likely that some calcium is still available for stabilizing some alginate chains into microscopic hydrogels or that some degree of chemical crosslinking occurred but at levels insufficient to preserve the integrity of the bulk hydrogel.

This level of tissue fixation is not suitable for situations where entire constructs are to be imaged histologically and likely explains previous reports of near complete dissolution of calcium alginate beads with NBF (McGowan and Nagatomi, 2013). Nonetheless, we and others have successfully used NBF to fix larger calcium alginate hydrogels transplanted into animals using fixation times of hours to overnight fixation, depending on tissue thickness (Bochenek et al., 2018; Somo et al., 2020; De Santis et al., 2021). Our current data indicates that this macroscopic level of preservation is likely due to the ability of NBF to more readily utilize extracellular matrix and other proteins deposited by infiltrating cells to retain the general explant structure. Despite the appearance of successful fixation, previous studies have shown clear separation of transplanted microspheres from the neighboring transplanted tissue, as well as empty cavities surrounded by tissue (Bochenek et al., 2018; Somo et al., 2020) as we have observed here with cells encapsulated in the hydrogels. These empty regions in the histological sections may thus be locations where transplanted microspheres were retained and successfully isolated from a negative immune response and thus did not integrate with the tissue and allow for crosslinking of hydrogels to tissue or cells. We observed similar artefacts in our histological samples when PFA_Ca was used. Future studies, which are ideally coupled to the latest advances using non-invasive *in vivo* imaging approaches (Arifin et al., 2019; Patrick et al., 2020), are needed to carefully correlate histological level evidence of transplanted calcium alginate with the *in vivo* scenario. It will thus be of particular interest to evaluate if FF fixation of ionically crosslinked calcium alginate also performs better than formalin-based fixatives in the *in vivo* setting.

The FF used here is a proprietary formulation and therefore we can only partially speculate on the mechanism by which it preserves the structure of calcium alginate hydrogels as well as cell-biomaterial interactions. The FF contains ethanol at concentrations greater than >30%, but the exact concentration is not known. The minimum concentration which is needed for tissue fixation of calcium alginate is not known, but several other studies exploring alcohol-based fixation report values of around 70% as optimal for alcohol-based fixation of native tissues (Panzacchi et al., 2019). Based on our previous experience, immersion of calcium alginate hydrogels fixed with NBF for 1 h caused their disintegration when placed into 30% ethanol for longer than 2 h (*data not shown*). Therefore, we speculate that the higher concentration of ethanol reported for the FF formulation (i.e., 50-60% ethanol) or additional components in FF help stabilize the calcium alginate hydrogels during tissue processing. Interestingly, we observed that the FF had an acidic pH (<4) which is known to also be used in some fixatives reported for native tissues (Varro and Brinkmann, 1990; Howat and Wilson, 2014; Stefanits et al., 2016). Therefore, it is possible that these two coagulative/denaturing agents work together to achieve tissue fixation. However, we cannot exclude the possibility that another additive at low concentrations may be responsible for the main fixative or stabilization we have observed which allows for retention of calcium alginate hydrogels during tissue processing. Interestingly, ethanol-based fixation has previously been shown to cause tissue shrinkage (Moelans et al., 2011). Thus, other additives such as trehalose, glycerin and glycerol have been added in other reported formulations to reduce tissue level shrinkage (Perry et al., 2016; Stefanits et al., 2016; Hewitt, 2017). It will be important to compare these other commercially available and laboratory made fixatives, which are alcohol based, to see if they are able to perform comparably or better than the FF used here.

Despite the fact that identification and implementation of formalin-free alternatives has been identified as a main goal in histological processing for the last 20 years, there has been slow adaptation of alternatives due to the need to re-validate antibodies with these fixatives (Moelans et al., 2011; Stefanits et al., 2016; Rahman et al., 2022). Alcohol-based fixatives have emerged as promising alternatives, but their slow adoption has thus led to the removal of some products from the market due to low-volume sales. This market instability has made it even less attractive for researchers to switch to these more environmentally and occupationally friendly and sustainable approaches (Zanini et al., 2012). Therefore, formulations with fully disclosed components are important to identify to ensure that it remains attractive and sustainable for researchers to move towards more environmentally friendly alternatives. Furthermore, there is very limited data as to the efficacy of these alternatives in tissue engineering approaches which have different chemical moieties and potential structures available for fixation. While UV-Vis spectroscopy can provide insights into

structural changes inferred from changes in optical absorption, a main limitation of the current work is a lack of chemical characterization of the mechanism of fixation (i.e., bonds formed during fixation). It will be important in future work to further characterize the mechanism of fixation using additional analytical approaches such as Fourier Transform-Infrared Spectroscopy (FT-IR) and nuclear magnetic resonance (NMR). However, such characterization should be performed in the hydrated state in order to avoid alterations in the infrared (IR) spectra known to be caused from histological processing. (Zohdi et al., 2015; Gvazava et al., 2023). This has previously been challenging to achieve with traditional IR approaches due to the absorption of water in IR ranges of interest for biological molecules. However, we have recently demonstrated the potential for performing infrared spectroscopy on hydrated native tissue biopsies using an optical photothermal infrared (O-PTIR) approach which eliminates the need for sample preparation. (Zohdi et al., 2015; Gvazava et al., 2023). Thus, emerging techniques which allow non-invasive "live" approaches in hydrated samples, such as O-PTIR, that do not require extensive sample preparation, may hold promise to better understand and evaluate the fixation process of hydrogels in chemical crosslinking *versus* coagulation/denaturing fixation. This will be important to pursue in future studies.

While we have evaluated the potential of one formalin-free alternative, additional work should be undertaken with FF and other alcohol-based laboratory fixatives (Rahman et al., 2022) using more advanced manufacturing methods, such as 3D bioprinting, to explore the potential of alcohol based fixatives for histological evaluation of more structurally complex hydrogel-based tissue engineering approaches (Koch and Włodarczyk-Biegun, 2020). One major benefit of the FF approach described here is the possibility to perform parallel observation using epitope-labelling microscopy techniques and SEM concurrently from the same sample, something which is not readily done with samples prepared with glutaraldehyde-based fixation due to heavy crosslinking of protein (Richards and Knowles, 1968). Preservation of hydrogel structures for visualization in conventional SEM is known to be challenging and thus our findings represent a new potential application for FF in evaluating hydrogels using SEM. Cryo-SEM is commonly used due to the fact that it prevents architectural deformation due to dehydration, but temperature control is of the highest importance as samples need to be cooled quickly to below the water glass-transition temperature (−137°C) to prevent artefacts in the form of crystalline formation (Aston et al., 2016; Lucas et al., 2022). Thus, future studies should compare hydrogel structures processed using FF preparations and evaluated in parallel using cryo-SEM. The ability to readily visualize hydrogels using conventional SEM would be a major advance as specialized equipment, storage, and a highly-trained personnel is needed for cryo-SEM compared to regular SEM imaging. Finally, alcohol-based fixatives such as the FF we used here have been shown to better preserve epitopes for immunohistochemical based analysis (van Essen et al., 2010). Future work should therefore evaluate the compatibility of the entire formalin-free and xylene-free workflow to ensure that immunofluorescent staining of cells in biomaterial hydrogels is still feasible.

In conclusion, our data indicates that FF and potentially more broadly, alcohol-acid based formalin free fixatives, hold promise for use in evaluating ionically crosslinked calcium alginate-based hydrogels used as tissue engineering scaffolds, for cell encapsulation and cell therapy, as well as drug delivery agents. Furthermore, this class of fixatives removes the use of formalin which is a known carcinogen and environmental pollutant. Encouragingly, we found that FF based fixation creates constructs which are also stable enough to be used in xylene-free tissue processing protocols and under the conditions of vacuum in SEM. Thus, the combination of FF and xylene free tissue processing is an important advance which will allow the further exploration of the naturally-sourced biomaterial, sodium alginate, to be validated and evaluated using green histological approaches to better understand its potential to be translated towards the clinic for diverse applications.

Data availability statement

The raw data supporting the conclusions of this article will be made available by the authors, without undue reservation.

Ethics statement

The animal study was reviewed and approved by Malmö/Lund Ethics Committee on Animal Testing.

Author contributions

IS and DEW conceptualized the project. IS, NG, IPW, RG, FG, OK, and DEW designed methodology. RG and DEW wrote software and performed data curation. IS, NG, IPW, RG and DEW performed validation studies within this work. IS, NG, IPW, RG, JS, OK, and DEW performed formal analysis. IS, NG, IPW, RG, and DEW performed experiments. JS, OK, and DEW provided resources. JS, OK, and DEW performed supervision. DEW oversaw project administration and acquired funding. IS, NG, IPW, RG, and DEW wrote the original draft. All authors participated in reviewing and editing the manuscript and approved the final submitted version.

Funding

This project has received funding from the European Research Council (ERC) under the European Union's Horizon 2020 research and innovation programme (grant agreement No 805361) (DEW). The Knut and Alice Wallenberg foundation, the Medical Faculty at Lund University, and Region Skåne are acknowledged for financial support (DEW). Lund University and the Strategic Research Area "Emerging Research Topics" are also acknowledged for support (DEW and OK).

Acknowledgments

The authors wish to thank all current and previous LBR members for their contribution to the evolution of this project by identifying bottlenecks in previous experiments and in trial experiments evaluating alternative fixatives to identify sustainable and environmentally friendly alternatives for histological processing. The authors are grateful to Hani Alsafadi for assistance in 3D printing and Jimena RG for assistance in

optimizing contour plots for improved visualization. We are particularly grateful to the input and technical assistance from Sebastian Wassterstrom at the Lund Bioimaging Center for acquisition of the scanning electron microscopy images as well as Lina Gefors for helpful conversations throughout the evolution of this project regarding the history of the search for more occupationally and environmentally safe alternatives for histological processing and electron microscopy preparation.

Conflict of interest

The authors declare that the research was conducted in the absence of any commercial or financial relationships that could be construed as a potential conflict of interest.

Publisher's note

Supplementary material

The Supplementary Material for this article can be found online at: https://www.frontiersin.org/articles/10.3389/fbiom.2023.1155919/full#supplementary-material

References

Abasalizadeh, F., Moghaddam, S. V., Alizadeh, E., Akbari, E., Kashani, E., Fazljou, S. M. B., et al. (2020). Alginate-based hydrogels as drug delivery vehicles in cancer treatment and their applications in wound dressing and 3D bioprinting. *J. Biol. Eng.* 14, 8. doi:10.1186/s13036-020-0227-7

Aderibigbe, B. A., and Buyana, B. (2018). Alginate in wound dressings. *Pharmaceutics* 10, 42. [Online]. doi:10.3390/pharmaceutics10020042

Alsafadi, H. N., Stegmayr, J., Ptasinski, V., Silva, I., Mittendorfer, M., Murray, L. A., et al. (2022). Simultaneous isolation of proximal and distal lung progenitor cells from individual mice using a 3D printed guide reduces proximal cell contamination of distal lung epithelial cell isolations. *Stem Cell Rep.* 17, 2718–2731. doi:10.1016/j.stemcr.2022.11.002

Argenta, D. F., Dos Santos, T. C., Campos, A. M., and Caon, T. (2019). "Chapter 3 - hydrogel nanocomposite systems: Physico-chemical characterization and application for drug-delivery Systems**Dedicated to professor claudia maria oliveira simões on the occasion of her retirement," in *Nanocarriers for drug delivery*. Editors S. S. MOHAPATRA, S. RANJAN, N. DASGUPTA, R. K. MISHRA, and S. THOMAS (Elsevier).

Arifin, D. R., Kulkarni, M., Kadayakkara, D., and Bulte, J. W. M. (2019). Fluorocapsules allow *in vivo* monitoring of the mechanical stability of encapsulated islet cell transplants. *Biomaterials* 221, 119410. doi:10.1016/j.biomaterials.2019.119410

Aston, R., Sewell, K., Klein, T., Lawrie, G., and Grøndahl, L. (2016). Evaluation of the impact of freezing preparation techniques on the characterisation of alginate hydrogels by cryo-SEM. *Eur. Polym. J.* 82, 1–15. doi:10.1016/j.eurpolymj.2016.06.025

Bajpai, M., Shukla, P., and Bajpai, S. K. (2017). Enhancement in the stability of alginate gels prepared with mixed solution of divalent ions using a diffusion through dialysis tube (DTDT) approach. *J. Macromol. Sci. Part A* 54, 301–310. doi:10.1080/10601325.2017.1294452

Bettinger, C. J., Zhang, Z., Gerecht, S., Borenstein, J. T., and Langer, R. (2008). Enhancement of *in vitro* capillary tube formation by substrate nanotopography. *Adv. Mater* 20, 99–103. doi:10.1002/adma.200702487

Bochenek, M. A., Veiseh, O., Vegas, A. J., Mcgarrigle, J. J., Qi, M., Marchese, E., et al. (2018). Alginate encapsulation as long-term immune protection of allogeneic pancreatic islet cells transplanted into the omental bursa of macaques. *Nat. Biomed. Eng.* 2, 810–821. doi:10.1038/s41551-018-0275-1

Caliari, S. R., and Burdick, J. A. (2016). A practical guide to hydrogels for cell culture. *Nat. Methods* 13, 405–414. doi:10.1038/nmeth.3839

Cammalleri, V., Pocino, R. N., Marotta, D., Protano, C., Sinibaldi, F., Simonazzi, S., et al. (2022). Occupational scenarios and exposure assessment to formaldehyde: A systematic review. *Indoor Air* 32, e12949. doi:10.1111/ina.12949

Cao, N., Chen, X. B., and Schreyer, D. J. (2012). Influence of calcium ions on cell survival and proliferation in the context of an alginate hydrogel. *ISRN Chem. Eng.* 2012, 516461–516469. doi:10.5402/2012/516461

De Haan, B. J., Van Goor, H., and De Vos, P. (2002). Processing of immunoisolated pancreatic islets: Implications for histological analyses of hydrated tissue. *Biotechniques* 32, 612-4, 616–618-9. doi:10.2144/02323rr03

De Santis, M. M., Alsafadi, H. N., Tas, S., Bölükbas, D. A., Prithiviraj, S., Da Silva, I. a. N., et al. (2021). Extracellular-matrix-reinforced bioinks for 3D bioprinting human tissue. *Adv. Mater.* 33, 2005476. doi:10.1002/adma.202005476

Dorozhkin, S. V. (2016). Calcium orthophosphates (CaPO4): Occurrence and properties. *Prog. Biomater.* 5, 9–70. doi:10.1007/s40204-015-0045-z

Fritschy, W. M., Gerrits, P. O., Wolters, G. H., Pasma, A., and Van Schilfgaarde, R. (1995). Glycol methacrylate embedding of alginate-polylysine microencapsulated pancreatic islets. *Biotech. Histochem* 70, 188–193. doi:10.3109/10520299509107311

Gepp, M. M., Fischer, B., Schulz, A., Dobringer, J., Gentile, L., Vásquez, J. A., et al. (2017). Bioactive surfaces from seaweed-derived alginates for the cultivation of human stem cells. *J. Appl. Phycol.* 29, 2451–2461. doi:10.1007/s10811-017-1130-6

Gerrits, P. O., Eppinger, B., Vangoor, H., and Horobin, R. (1991). A versatile, low toxicity glycol methacrylate embedding medium for use in biological-resarch, and for recovered biomaterials prostheses. *Cells Mater.* 1, 189–198.

Guillaume, O., Naqvi, S. M., Lennon, K., and Buckley, C. T. (2014). Enhancing cell migration in shape-memory alginate–collagen composite scaffolds: *In vitro* and *ex vivo* assessment for intervertebral disc repair. *J. Biomaterials Appl.* 29, 1230–1246. doi:10.1177/0885328214557905

Gvazava, N., Konings, S., Cepeda-Prado, E., Skoryk, V., Umeano, C., Dong, J., et al. (2023). Label-free high-resolution infrared spectroscopy for spatiotemporal analysis of complex living systems. *bioRxiv*. doi:10.1101/2023.01.05.522847

Hewitt, S. M. (2017). Formulation and pH of the buffered ethanol fixative BE70. *J. Histochem. Cytochem.* 65, 251–252. doi:10.1369/0022155416687279

Hoffman, A. S. (2012). Hydrogels for biomedical applications. *Adv. Drug Deliv. Rev.* 64, 18–23. doi:10.1016/j.addr.2012.09.010

Howat, W. J., and Wilson, B. A. (2014). Tissue fixation and the effect of molecular fixatives on downstream staining procedures. *Methods* 70, 12–19. doi:10.1016/j.ymeth.2014.01.022

Hunt, N. C., Shelton, R. M., and Grover, L. M. (2009). Reversible mitotic and metabolic inhibition following the encapsulation of fibroblasts in alginate hydrogels. *Biomaterials* 30, 6435–6443. doi:10.1016/j.biomaterials.2009.08.014

Jacobs-Tulleneers-Thevissen, D., Chintinne, M., Ling, Z., Gillard, P., Schoonjans, L., Delvaux, G., et al. (2013). Sustained function of alginate-encapsulated human islet cell implants in the peritoneal cavity of mice leading to a pilot study in a type 1 diabetic patient. *Diabetologia*, 56, 1605–1614. doi:10.1007/s00125-013-2906-0

Jain, M., Ngoy, S., Sheth, S. A., Swanson, R. A., Rhee, E. P., Liao, R., et al. (2014). A systematic survey of lipids across mouse tissues. *Am. J. Physiol. Endocrinol. Metab.* 306, E854–E868. doi:10.1152/ajpendo.00371.2013

James, R., Jenkins, L., Ellis, S. E., and Burg, K. J. L. (2004). Histological processing of hydrogel scaffolds for tissue-engineering applications. *J. Histotechnol.* 27, 133–139. doi:10.1179/his.2004.27.2.133

Jeon, O., Lee, Y. B., Hinton, T. J., Feinberg, A. W., and Alsberg, E. (2019). Cryopreserved cell-laden alginate microgel bioink for 3D bioprinting of living tissues. *Mater. Today Chem.* 12, 61–70. doi:10.1016/j.mtchem.2018.11.009

Johnson, A. S., O'sullivan, E., D'aoust, L. N., Omer, A., Bonner-Weir, S., Fisher, R. J., et al. (2011). Quantitative assessment of islets of Langerhans encapsulated in alginate. *Tissue Eng. Part C Methods* 17, 435–449. doi:10.1089/ten.tec.2009.0510

Julian, T. N., Radebaugh, G. W., and Wisniewski, S. J. (1988). Permeability characteristics of calcium alginate films. *J. Control. Release* 7, 165–169. doi:10.1016/0168-3659(88)90008-9

Khatab, S., Leijs, M. J., Van Buul, G., Haeck, J., Kops, N., Nieboer, M., et al. (2020). MSC encapsulation in alginate microcapsules prolongs survival after intra-articular injection, a longitudinal *in vivo* cell and bead integrity tracking study. *Cell Biol. Toxicol.* 36, 553–570. doi:10.1007/s10565-020-09532-6

Kiernan, J. A. (2000). Formaldehyde, formalin, paraformaldehyde and glutaraldehyde: What they are and what they do. *Microsc. Today* 8, 8–13. doi:10.1017/s1551929500057060

Koch, M., and Włodarczyk-Biegun, M. K. (2020). Faithful scanning electron microscopic (SEM) visualization of 3D printed alginate-based scaffolds. *Bioprinting* 20, e00098. doi:10.1016/j.bprint.2020.e00098

Kuo, C. K., and Ma, P. X. (2008). Maintaining dimensions and mechanical properties of ionically crosslinked alginate hydrogel scaffolds *in vitro*. *J. Biomed. Mater. Res. Part A* 84A, 899–907. doi:10.1002/jbm.a.31375

Lee, K. Y., and Mooney, D. J. (2012). Alginate: Properties and biomedical applications. *Prog. Polym. Sci.* 37, 106–126. doi:10.1016/j.progpolymsci.2011.06.003

Lee, K., Choi, S., Yang, C., Wu, H.-C., and Yu, J. (2013). Autofluorescence generation and elimination: A lesson from glutaraldehyde. *Chem. Commun.* 49, 3028–3030. doi:10.1039/c3cc40799c

Li, J., Wu, Y., He, J., and Huang, Y. (2016). A new insight to the effect of calcium concentration on gelation process and physical properties of alginate films. *J. Mater. Sci.* 51, 5791–5801. doi:10.1007/s10853-016-9880-0

Lucas, P., Pries, J., Wei, S., and Wuttig, M. (2022). The glass transition of water, insight from phase change materials. *J. Non-Cryst. Solids* X, 14. doi:10.1016/j.nocx.2022.100084

Mcgowan, B. H., and Nagatomi, J. (2013). Histological techniques for preservation of alginate bead structural integrity using glycolmethacrylate. *J. Histotechnol.* 36, 100–105. doi:10.1179/2046023613y.0000000029

Metgud, R., Astekar, M. S., Soni, A., Naik, S., and Vanishree, M. (2013). Conventional xylene and xylene-free methods for routine histopathological preparation of tissue sections. *Biotech. Histochem.* 88, 235–241. doi:10.3109/10520295.2013.764015

Moelans, C. B., Ter Hoeve, N., Van Ginkel, J. W., Ten Kate, F. J., and Van Diest, P. J. (2011). Formaldehyde substitute fixatives. Analysis of macroscopy, morphologic analysis, and immunohistochemical analysis. *Am. J. Clin. Pathol.* 136, 548–556. doi:10.1309/ajcphh1b0cocbgom

Mørch, Y. A., Donati, I., Strand, B. L., and Skjåk-Braek, G. (2006). Effect of Ca2+, Ba2+, and Sr2+ on alginate microbeads. *Biomacromolecules* 7, 1471–1480. doi:10.1021/bm060010d

Neves, M. I., Moroni, L., and Barrias, C. C. (2020). Modulating alginate hydrogels for improved biological performance as cellular 3D microenvironments. *Front. Bioeng. Biotechnol.* 8, 665. doi:10.3389/fbioe.2020.00665

Nicodemus, G. D., and Bryant, S. J. (2008). Cell encapsulation in biodegradable hydrogels for tissue engineering applications. *Tissue Eng. Part B Rev.* 14, 149–165. doi:10.1089/ten.teb.2007.0332

Panzacchi, S., Gnudi, F., Mandrioli, D., Montella, R., Strollo, V., Merrick, B. A., et al. (2019). Effects of short and long-term alcohol-based fixation on Sprague-Dawley rat tissue morphology, protein and nucleic acid preservation. *Acta Histochem.* 121, 750–760. doi:10.1016/j.acthis.2019.05.011

Patrick, P. S., Bear, J. C., Fitzke, H. E., Zaw-Thin, M., Parkin, I. P., Lythgoe, M. F., et al. (2020). Radio-metal cross-linking of alginate hydrogels for non-invasive *in vivo* imaging. *Biomaterials* 243, 119930. doi:10.1016/j.biomaterials.2020.119930

Perry, C., Chung, J. Y., Ylaya, K., Choi, C. H., Simpson, A., Matsumoto, K. T., et al. (2016). A buffered alcohol-based fixative for histomorphologic and molecular applications. *J. Histochem. Cytochem.* 64, 425–440. doi:10.1369/0022155416649579

Rahman, M. A., Sultana, N., Ayman, U., Bhakta, S., Afrose, M., Afrin, M., et al. (2022). Alcoholic fixation over formalin fixation: A new, safer option for morphologic and molecular analysis of tissues. *Saudi J. Biol. Sci.* 29, 175–182. doi:10.1016/j.sjbs.2021.08.075

Rajan, S., and Malathi, N. (2014). Health hazards of xylene: A literature review. *J. Clin. Diagn Res.* 8, 271–274. doi:10.7860/JCDR/2014/7544.4079

Rastogi, P., and Kandasubramanian, B. (2019). Review of alginate-based hydrogel bioprinting for application in tissue engineering. *Biofabrication* 11, 042001. doi:10.1088/1758-5090/ab331e

Richards, F. M., and Knowles, J. R. (1968). Glutaraldehyde as a protein cross-linking reagent. *J. Mol. Biol.* 37, 231–233. doi:10.1016/0022-2836(68)90086-7

Rowley, J. A., Madlambayan, G., and Mooney, D. J. (1999). Alginate hydrogels as synthetic extracellular matrix materials. *Biomaterials* 20, 45–53. doi:10.1016/s0142-9612(98)00107-0

Schoephoerster, R. T., Wertz, P. W., Madison, K. C., and Downing, D. T. (1985). A survey of polar and non-polar lipids of mouse organs. *Comp. Biochem. Physiol. Part B Comp. Biochem.* 82, 229–232. doi:10.1016/0305-0491(85)90231-7

Segale, L., Giovannelli, L., Mannina, P., and Pattarino, F. (2016). Calcium alginate and calcium alginate-chitosan beads containing celecoxib solubilized in a self-emulsifying phase. *Sci. (Cairo)* 2016, 1–8. doi:10.1155/2016/5062706

Silva, I. a. N., Gvazava, N., Bolukbas, D. A., Stenlo, M., Dong, J., Hyllen, S., et al. (2022). A semi-quantitative scoring system for green histopathological evaluation of large animal models of acute lung injury. *Bio Protoc.* 12, e4493. doi:10.21769/bioprotoc.4493

Somo, S. I., Brown, J. M., and Brey, E. M. (2020). Dual crosslinking of alginate outer layer increases stability of encapsulation system. *Front. Chem.* 8, 575278. doi:10.3389/fchem.2020.575278

Stefanits, H., Bienkowski, M., Galanski, M., Mitulovic, G., Ströbel, T., Gelpi, E., et al. (2016). KINFix--A formalin-free non-commercial fixative optimized for histological, immunohistochemical and molecular analyses of neurosurgical tissue specimens. *Clin. Neuropathol.* 35, 3–12. doi:10.5414/np300907

Tayri-Wilk, T., Slavin, M., Zamel, J., Blass, A., Cohen, S., Motzik, A., et al. (2020). Mass spectrometry reveals the chemistry of formaldehyde cross-linking in structured proteins. *Nat. Commun.* 11, 3128. doi:10.1038/s41467-020-16935-w

Temirel, M., Dabbagh, S. R., and Tasoglu, S. (2022). Shape fidelity evaluation of alginate-based hydrogels through extrusion-based bioprinting. *J. Funct. Biomaterials* 13, 225. [Online]. doi:10.3390/jfb13040225

Uyen, N. T. T., Hamid, Z. a. A., Tram, N. X. T., and Ahmad, N. (2020). Fabrication of alginate microspheres for drug delivery: A review. *Int. J. Biol. Macromol.* 153, 1035–1046. doi:10.1016/j.ijbiomac.2019.10.233

Van Essen, H. F., Verdaasdonk, M. A., Elshof, S. M., De Weger, R. A., and Van Diest, P. J. (2010). Alcohol based tissue fixation as an alternative for formaldehyde: Influence on immunohistochemistry. *J. Clin. Pathol.* 63, 1090–1094. doi:10.1136/jcp.2010.079905

Varro, A., and Brinkmann, B. (1990). Preservation of stab and cut wounds of the skin. *Arch. Kriminol.* 186, 159–162.

Wagner, D. E., Jones, A. D., Zhou, H., and Bhaduri, S. B. (2013). Cytocompatibility evaluation of microwave sintered biphasic calcium phosphate scaffolds synthesized using pH control. *Mater Sci. Eng. C Mater Biol. Appl.* 33, 1710–1719. doi:10.1016/j.msec.2012.12.084

Werner, M., Chott, A., Fabiano, A., and Battifora, H. (2000). Effect of formalin tissue fixation and processing on immunohistochemistry. *Am. J. Surg. Pathol.* 24, 1016–1019. doi:10.1097/00000478-200007000-00014

Yeom, C. K., and Lee, K. H. (1998). Characterization of sodium alginate membrane crosslinked with glutaraldehyde in pervaporation separation. *J. Appl. Polym. Sci.* 67, 209–219. doi:10.1002/(sici)1097-4628(19980110)67:2<209::aid-app3>3.0.co;2-y

Yeung, E. C., and Chan, C. K. W. (2014). Glycol methacrylate: The art of embedding and serial sectioning. *Botany* 93, 1–8. doi:10.1139/cjb-2014-0177

Zanini, C., Gerbaudo, E., Ercole, E., Vendramin, A., and Forni, M. (2012). Evaluation of two commercial and three home-made fixatives for the substitution of formalin: A formaldehyde–free laboratory is possible. *Environ. Health* 11, 59. doi:10.1186/1476-069x-11-59

Zohdi, V., Whelan, D. R., Wood, B. R., Pearson, J. T., Bambery, K. R., and Black, M. J. (2015). Importance of tissue preparation methods in FTIR micro-spectroscopical analysis of biological tissues: 'Traps for new users. *PLOS ONE* 10, e0116491. doi:10.1371/journal.pone.0116491